Adıyaman University Journal of Science
https://dergipark.org.tr/en/pub/adyujsci
DergiPark AKADEMİK
ISSN 2147-1630
e-ISSN 2146-586X

Synthesis, Surface Functionalization, and Characterization of $MoO_2(acac)_2$-Immobilized Magnetite Nanoparticles

Nastaran SADEGHIAN[1,2]*

[1] *Bartin University, Faculty of Science, Department of Biotechnology, 74110, Bartin, Turkey*
[2] *Islamic Azad University, Faculty of Chemistry, Ardabil branch, Ardabil, Iran*
nsadeghian@bartin.edu.tr, nastaranpar2015@yahoo.com, ,ORCID: 0009-0004-2966-9231

Received: 03.01.2026 **Accepted:** 08.06.2026 **Published:** 30.06.2026

Abstract

In this study, iron(II) and iron(III) salts were hydrolyzed alkalinely to create magnetite nanoparticles. Tetraethyl orthosilicate was hydrolyzed and condensed in the presence of magnetite to coat the resultant nanoparticles with a silica shell. An aminopropylsilane reagent was used to further modify the silica-coated magnetite nanoparticles in order to add functional amine groups to their surfaces. A coordination reaction was used in the last functionalization stage to immobilize a $MoO_2(acac)_2$ complex reported in the literature onto the amine-functionalized nanoparticles. Repeated water washing was used to get rid of extra chemicals. X-ray diffraction (XRD) and Fourier-transform infrared (FT-IR) spectroscopy verified the successful immobilization of $MoO_2(acac)_2$ on the magnetite surface. Transmission electron microscopy (TEM) was used to examine the morphological characteristics and particle size distribution of the produced nanoparticles, and vibrating sample magnetometry (VSM) was used to assess their magnetic behavior. The successful stability of the $MoO_2(acac)_2$ complex on the surface of magnetite nanoparticles is amply demonstrated by the characterization data.

Keywords: Magnetite Nanoparticle; $MoO_2(acac)_2$; Synthesis; Characterization.

* Corresponding Author DOI: 10.37094/adyujsci.1855068

$MoO_2(acac)_2$-İmmobilize Manyetit Nanoparçacıklarının Sentezi, Yüzey Fonksiyonelleştirilmesi ve Karakterizasyonu

Öz

Bu çalışmada, demir(II) ve demir(III) tuzları alkali hidroliz edilerek manyetit nanopartiküller oluşturulmuştur. Tetraetil ortosilikat, manyetit varlığında hidrolize edilmiş ve yoğunlaştırılmış, böylece elde edilen nanopartiküller silika kabukla kaplanmıştır. Silika kaplı manyetit nanopartiküllerin yüzeyine fonksiyonel amin grupları eklemek için aminopropilsilan reaktifi kullanılarak daha fazla modifikasyon yapılmıştır. Son fonksiyonelleştirme aşamasında, literatürde bildirilen bir $MoO_2(acac)_2$ kompleksinin aminle fonksiyonelleştirilmiş nanopartiküller üzerine immobilizasyonu için bir koordinasyon reaksiyonu kullanılmıştır. Fazla kimyasallardan kurtulmak için tekrarlanan su yıkama işlemi uygulanmıştır. X-ışını kırınımı (XRD) ve Fourier-transform kızılötesi (FT-IR) spektroskopisi, $MoO_2(acac)_2$'nin manyetit yüzeyine başarılı bir şekilde immobilizasyonunu doğrulamıştır. Üretilen nanopartiküllerin morfolojik özelliklerini ve partikül boyut dağılımını incelemek için transmisyon elektron mikroskobu (TEM) ve manyetik davranışlarını değerlendirmek için titreşimli numune manyetometresi (VSM) kullanılmıştır. Karakterizasyon verileri, $MoO_2(acac)_2$ kompleksinin manyetit nanopartiküllerinin yüzeyinde başarılı bir şekilde kararlı olduğunu açıkça göstermektedir.

Anahtar Kelimeler: Manyetit nanopartikül; $MoO_2(acac)_2$; sentez; karakterizasyon.

1. Introduction

Magnetic nanoparticles (MNPs) constitute an important class of nanomaterials whose physical and chemical properties can be precisely controlled by an external magnetic field. Owing to their unique features, including intrinsic magnetism, nanoscale dimensions, high surface-to-volume ratio, and generally low toxicity, MNPs have attracted considerable attention in both fundamental research and technological applications [1,2]. These materials are commonly composed of transition metals such as iron, cobalt, and nickel, with iron-based nanoparticles being the most extensively investigated due to their chemical stability and biocompatibility. As a result, magnetic nanoparticles have found widespread applications in diverse fields, including catalysis, biopharmaceuticals, magnetic resonance imaging (MRI), targeted drug delivery, data storage technologies, and environmental remediation. Among iron-based magnetic materials, mixed iron oxide (Fe_3O_4), commonly known as magnetite, is one of the most prominent and naturally occurring iron oxides. Magnetite possesses a mixed-valence structure containing both Fe^{2+} and Fe^{3+} ions and is often represented as $FeO \cdot Fe_2O_3$ [3,4]. In laboratory conditions, Fe_3O_4 is typically obtained as a black powder exhibiting superparamagnetic behavior at the nanoscale, a property

that is highly desirable for biomedical and catalytic applications due to the absence of remanent magnetization. In terms of structure, Fe_3O_4 nanoparticles crystallize in an inverse spinel structure with a face-centered cubic (fcc) lattice made up of an oxide ion arrangement that is cubic and closely packed. In this arrangement, half of the octahedral sites are occupied by Fe^{2+} ions, and the remaining octahedral and tetrahedral sites are occupied by Fe^{3+} ions. This unique cation distribution is responsible for the remarkable magnetic properties of magnetite nanoparticles and plays a crucial role in their performance in functional applications [5,6].

One of the most readily accessible precursor complexes for the synthesis of various molybdenum-based compounds is the emerald-green pentachlorooxomolybdate(V) ion, $[MoOCl_5]^{2-}$. This complex can be prepared either by the reduction of MoO_4^{2-} in hydrochloric acid medium or by dissolving $Mo_2O_5Cl_{10}$ in concentrated hydrochloric acid. Paramagnetic salts, such as $K_2[MoOCl_5]$, can be isolated from acidic solutions through controlled addition of hydroxide ions [7,8]. The red–brown species is representative of a common class of molybdenum(VI) oxo compounds. In order to develop biomimetic models for molybdoenzymes, particularly xanthine oxidase, various molybdenum complexes incorporating biologically relevant ligands such as amino acids, cysteine, and other sulfur-containing compounds have been extensively investigated. Notable examples include the xanthate complex with the composition $Mo_2O_3(S_2COEt)_4$ and a histidine-based complex formulated as $(L\text{-}His)_2{\cdot}3H_2O{\cdot}MoO_4$ [9,10].

Molybdenum is an essential trace element that plays a critical role in numerous biologically important oxidation–reduction enzymes and is unique among second-row transition metals in being indispensable for life. In biological systems, molybdenum is primarily absorbed as the molybdate anion and is obtained through dietary and environmental sources such as food, soil, and water. While adequate molybdenum levels are necessary for normal growth and metabolic function particularly in plants, deficiency leads to growth defects, and excessive intake can disrupt metal homeostasis, as observed in ruminants where molybdenum induces copper deficiency through the formation of stable Mo–S–Cu complexes [11]. Among molybdenum-dependent enzymes, nitrogenase is of particular significance due to its role in biological nitrogen fixation, catalyzing the reduction of atmospheric dinitrogen (N_2) to ammonia (NH_3). This enzyme consists of two oxygen-sensitive protein components: the iron–molybdenum (MoFe) protein, which contains molybdenum, iron, and sulfur atoms, and the iron protein, which functions as an electron donor. Mechanistic studies indicate that N_2 binds directly to a reduced molybdenum center within the MoFe protein, receiving electrons that are transferred from ferredoxin via the iron protein in an ATP-dependent process, ultimately facilitating N_2 protonation and reduction to NH_3 with H_2

as a by-product. Structural investigations suggest a closely coupled Fe–Mo–S cluster architecture that enables efficient multi-electron transfer during catalysis [12,13].

Molybdenum (Fig. 1) possesses several stable isotopes along with twelve known radioactive isotopes, among which ^99Mo is of particular importance due to its use in generator systems for the production of ^99mTc, a key radionuclide in nuclear medicine and the radioisotope industry. Molybdenum-containing minerals readily undergo decomposition in solution and can precipitate as sulfide phases in the presence of heavy metals, even under relatively pure conditions [14,15]. Positioned as the second element in Group 6 of the periodic table, molybdenum is a transition metal that exhibits multiple oxidation states, most commonly +2, +3, +4, +5, and +6. In its bulk metallic form, molybdenum displays typical metallic characteristics with a bright silvery-white appearance, whereas in powdered form it appears dark gray. The physical properties of molybdenum are strongly influenced by its method of production and degree of purification; for instance, its reported density varies in the range of 9.01–10.22 $g \cdot cm^{-3}$. Notably, molybdenum does not occur in its elemental form in nature, but it is found in various mineral compounds [16,17].

The aim of this study is to synthesize silica-coated and amine-functionalized magnetite nanoparticles and to immobilize the $MoO_2(acac)_2$ complex onto their surface. The work further seeks to confirm the successful surface functionalization and stabilization of the molybdenum complex through comprehensive structural and spectroscopic characterization. Additionally, the morphological and magnetic properties of the resulting nanomaterials are systematically investigated.

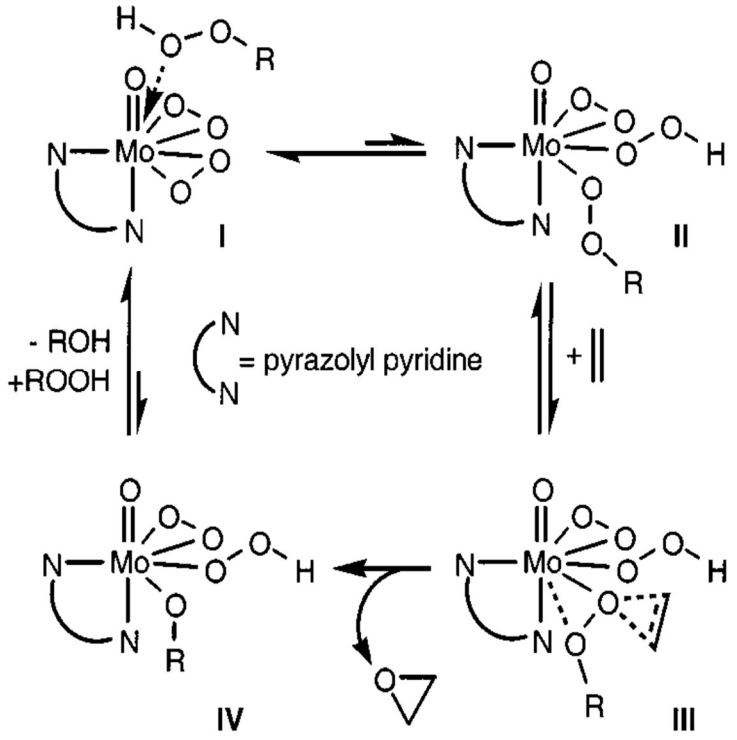

Figure 1: Hydroperoxide activity in the molybdenum peroxo coordination space

2. Material and Methods

2.1. Instruments

A PerkinElmer RXI FT-IR 2400 spectrometer was used to record the samples' Fourier-transform infrared (FT-IR) spectra. The samples were produced as KBr pellets. Cu Kα radiation was used on a Rigaku D/MAX-C III diffractometer to obtain X-ray diffraction (XRD) patterns. A Philips EM 208S microscope running at an accelerating voltage of 100 kV was used to obtain transmission electron microscopy (TEM) images. A Zeiss DSM 960A microscope was used to gather scanning electron microscopy (SEM) pictures.

2.2. Synthesis of Magnetite Nanoparticles (MNPs)

Magnetite nanoparticles were synthesized by a co-precipitation method. Briefly, 15.2 g of $FeCl_2 \cdot 4H_2O$ and 84.5 g of $FeCl_3 \cdot 6H_2O$ were dissolved in 80 mL of deionized water in a 250 mL beaker, resulting in an orange-colored solution. The mixture was stirred for 15 min until complete dissolution of the salts was achieved. Subsequently, 10 mL of 25% ammonia solution (Merck) was added dropwise under continuous stirring. The formation of a black precipitate was observed immediately upon the addition of ammonia, and precipitation was completed when the pH reached 9. After that, the reaction mixture was kept at 80–90 °C and agitated for a further half

hour. A powerful external magnet was used to separate the resultant magnetite nanoparticles, which were then cleaned twice with deionized water and once with a 2% NaCl solution. Vibrating sample magnetometry (VSM) and FT-IR spectroscopy were used to characterize the produced iron oxide nanoparticles [18,19].

2.3. Preparation of Silica-Coated Magnetite Nanoparticles (SCMNPs)

The as-prepared magnetite nanoparticles were dispersed in a beaker, followed by the addition of 16 mL of tetraethyl orthosilicate (TEOS, 20% v/v) and 200 mL of glycerol. The pH of the suspension was adjusted to 4.5 using glacial acetic acid. Nitrogen gas was bubbled through the mixture for 15 min to create an inert atmosphere, after which the system was maintained under a nitrogen atmosphere using a balloon. The mixture was refluxed for two hours after the reaction temperature was increased to 90 °C. Once the reaction was finished, the supernatant was decanted and the silica-coated magnetite nanoparticles were gathered using a magnet. The precipitate was cleaned twice using deionized water and then either methanol or ethanol. This washing procedure was repeated three times to facilitate efficient drying of the product. After drying, a portion of the silica-coated nanoparticles was collected for spectroscopic characterization [20,21].

2.4. Modification of Silica-Coated Magnetite Nanoparticles with Aminopropyl Groups (APSMNPs)

Silica-coated magnetite nanoparticles were dispersed in 150 mL of a 2% (v/v) solution of aminopropylsilane in ethanol. The aminopropylsilane solution was prepared by mixing 12 mL of aminopropyltrimethoxysilane (APTS) with 300 mL of ethanol, followed by adjustment of the pH to 4.5 using glacial acetic acid. The reaction mixture was refluxed at 60 °C for 2 h under a nitrogen atmosphere maintained by a balloon. Upon completion of the reaction, the nanoparticles were separated using an external magnet, and the supernatant was decanted. The resulting precipitate was washed twice with double-distilled water and twice with methanol, then dried and used in subsequent functionalization steps [22].

2.5. Stabilization of Bis(acetylacetonato)dioxomolybdenum on the Surface of Magnetite Nanoparticles

In a 100 mL beaker, 0.65 g of bis(acetylacetonato)dioxomolybdenum, $MoO_2(acac)_2$, was dissolved in 50 mL of methanol under stirring. Subsequently, 1.0 g of amine-functionalized magnetite nanoparticles was added to the solution, and the resulting suspension was refluxed for 24 h. After completion of the reaction, the functionalized nanoparticles were collected using a strong external magnet, washed three times with methanol to remove unbound complexes, and

dried under vacuum [23, 24]. The final product was then prepared for spectroscopic characterization (Fig. 2).

Figure 2: Stabilization of Bis(acetylacetonato)dioxomolybdenum on the surface of magnetite nanoparticles

3. Results and Discussion

The overall synthesis of magnetite nanoparticles was performed using the co-precipitation method, employing iron(II) and iron(III) salts in a stoichiometric molar ratio of 1:2. Magnetite nanoparticles are sensitive to oxidation, and partial conversion to iron hydroxide species (e.g., $Fe(OH)_2$/$Fe(OH)_3$) may occur upon exposure to atmospheric oxygen.

3.1. FT-IR spectrum of magnetite nanoparticles

Figure 3 presents the FT-IR spectrum of the synthesized magnetite nanoparticles. The characteristic absorption bands corresponding to Fe–O stretching vibrations in the magnetite lattice were observed at 583 and 422 cm^{-1}. At the nanoscale, size confinement effects lead to the disruption of a significant number of surface atomic bonds, resulting in electron redistribution and partial delocalization at the nanoparticle surface. This phenomenon increases the surface bond force constant as the particle size decreases, causing the Fe–O vibrational bands to shift toward higher wavenumbers. Consequently, a blue shift in the FT-IR absorption bands is observed, which is indicative of the nanoscale dimensions of the Fe_3O_4 particles. Additionally, the broad absorption band around 3396 cm^{-1} and the band at 1624 cm^{-1} are attributed to the stretching and bending vibrations of surface hydroxyl (–OH) groups, respectively.

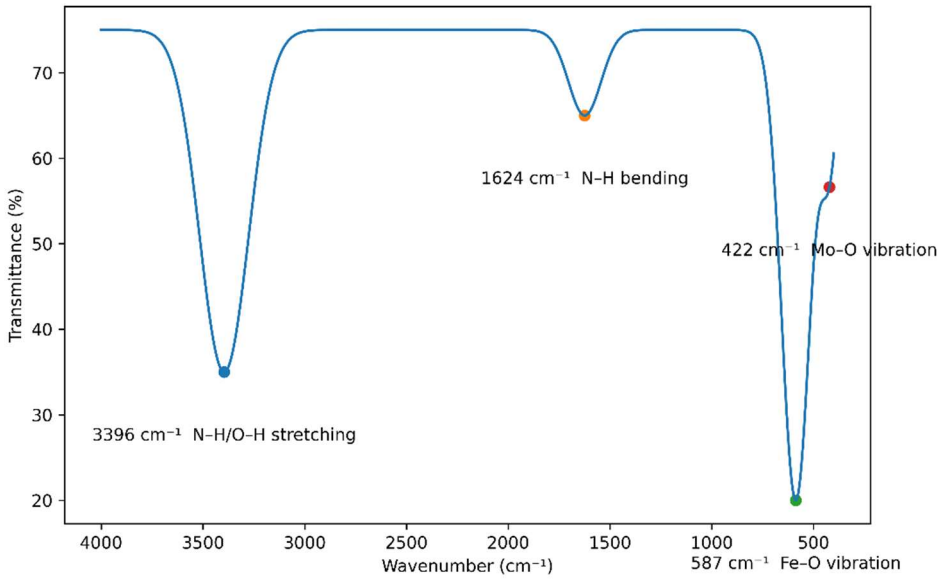

Figure 3: FT-IR spectrum of magnetite magnetic nanoparticles

3.2. Investigation of VSM analysis of magnetite nanoparticles

Vibrating sample magnetometry (VSM) was used to assess the magnetic characteristics of the produced nanoparticles. Fig. 4 shows the magnetization curve as a function of the applied magnetic field. The magnetization curve's lack of hysteresis suggests single-domain behavior, which validates the nanoparticles' superparamagnetic properties. The saturation magnetization was found to be at 60 emu·g^{-1}, which is consistent with values reported for nanostructured magnetite.

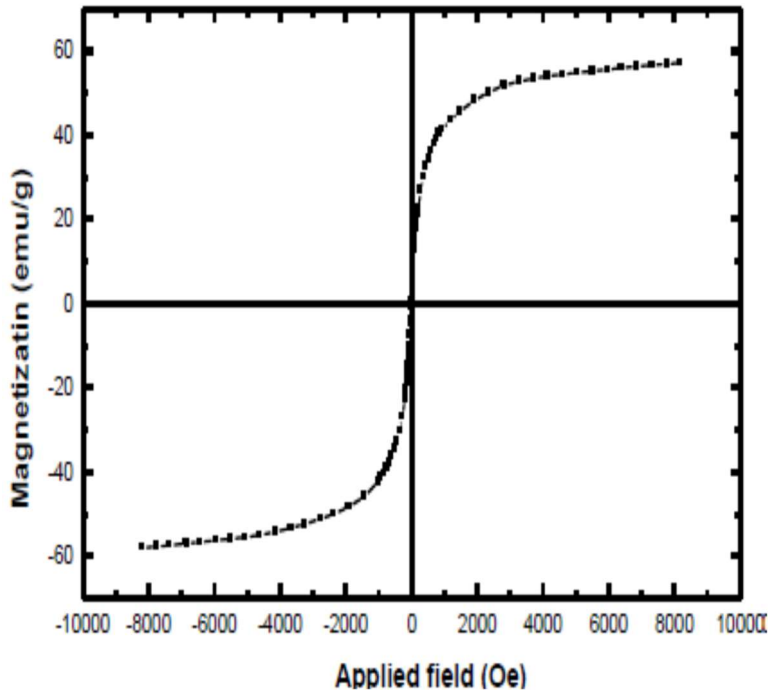

Figure 4: Magnetization curve versus field for nanomagnetite composition

3.3. Silica-coated magnetite nanoparticles (SCMNPS)

Tetraethyl orthosilicate (TEOS) was hydrolyzed and condensed to coat the magnetite nanoparticles produced in the first stage with a silica coating. The silica coating serves as an inert protective shell that isolates the metal oxide core from the reaction medium, thereby preventing undesirable surface reactions. In addition, the presence of a silica layer provides a suitable platform for further surface functionalization and enhances the thermal stability of the magnetite nanoparticles.

One of the most significant advantages of silica coating is the increased density of surface hydroxyl (–OH) groups compared to bare magnetite, which greatly facilitates subsequent chemical modification. Moreover, the silica shell improves the dispersibility of the nanoparticles in aqueous media. In this process, TEOS was introduced in the presence of glycerol and glacial acetic acid. Glycerol acts as a stabilizing medium, promoting effective separation of the magnetic nanoparticles and uniform deposition of the silica layer on their surfaces. The addition of acid adjusts the pH of the system, enabling efficient hydrolysis of both the surface hydroxyl groups of magnetite and the TEOS molecules, which in turn promotes strong interfacial bonding and uniform silica shell formation (Fig. 5).

Figure 5: Silica-coated magnetite nanoparticles

3.4. FT-IR Spectrum of Silica-Coated Magnetite Nanoparticles

Figure 6 displays the silica-coated magnetite nanoparticles' FT-IR spectra. Fe–O–Si interfacial connections show that a silica network has formed on the surface of the magnetite nanoparticles. Successful silica coating is confirmed by the distinctive absorption band at 1049 cm^{-1}, which is related to the asymmetric stretching vibration of Si–O–Si links.

The broad absorption band centered at 3391 cm^{-1} and the relatively sharp band at 1627 cm^{-1} correspond to the stretching and bending vibrations of O–H bonds, respectively, arising from surface-adsorbed water and hydroxyl groups. In addition, these features can be associated with hydrogen-bonded silanol (Si–OH) groups, which typically exhibit absorption in the 3200–3400 cm^{-1} region. The bands appearing at 587 and 449 cm^{-1} are characteristic of Fe–O vibrations within the magnetite core, indicating that the crystalline structure of Fe_3O_4 is preserved after silica coating.

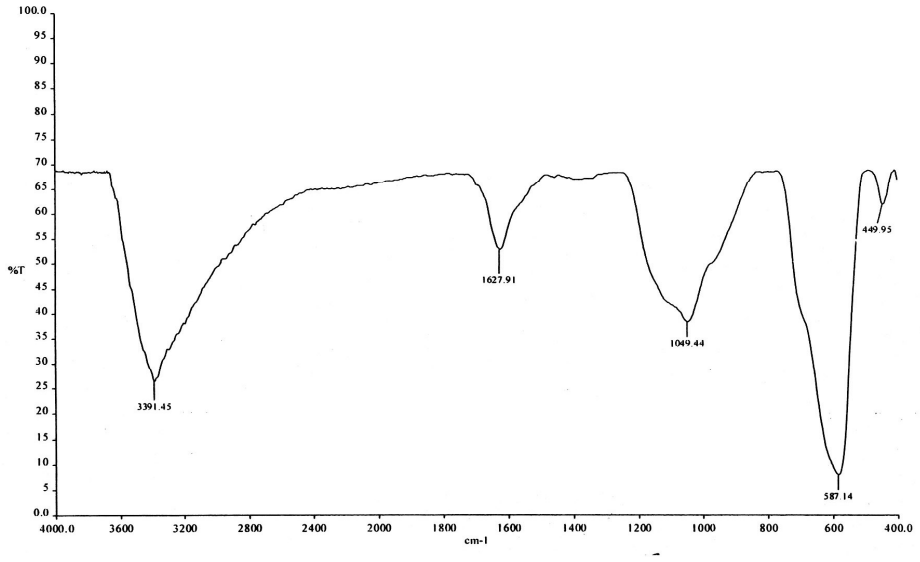

Figure 6: FT-IR spectrum of silica-coated magnetite nanoparticles

3.5. Silica-Coated Magnetite Nanoparticles Functionalized

3.5.1. Aminopropyltrimethoxysilane (APTS–SCMNPs)

3.5.1.1. Formation Mechanism

Surface functionalization of magnetite nanoparticles represents an effective strategy for modifying their external surfaces, enabling the immobilization of various functional molecules. Of particular interest is the attachment of inorganic or organometallic ligands to prepare heterogeneous catalysts supported on nanomagnetite. Among the commonly employed surface-modifying agents, aminopropyltrimethoxysilane (APTS) has been widely used due to its ability to introduce reactive amine groups.

The functionalization process proceeds through two main stages. In the first stage, APTS undergoes acid-catalyzed hydrolysis in an aqueous medium, during which the methoxy groups are converted into silanol (Si–OH) groups. The hydrolyzed species subsequently undergo condensation reactions, leading to the formation of siloxane networks. In the second stage, these hydrolyzed APTS species interact with the surface of silica-coated magnetite nanoparticles through condensation reactions between the silanol groups of APTS and the surface hydroxyl groups of the silica shell. This process results in the formation of stable covalent Si–O–Si bonds via surface dehydroxylation. The final product is obtained as a black, dense precipitate that exhibits strong magnetic responsiveness under an external magnetic field, confirming the successful functionalization of the silica-coated magnetite nanoparticles with aminopropyl groups (Fig. 7).

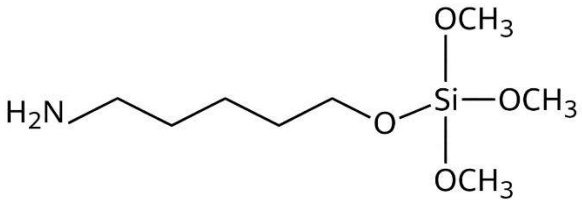

Figure 7: Structure of the Aminopropyltrimethoxysilane molecule

3.6. FT-IR Spectrum of Silica-Coated and APTS-Functionalized Magnetite Nanoparticles (APTS–SCMNPs)

The FT-IR spectrum of magnetite nanoparticles coated with silica and subsequently functionalized with aminopropyltrimethoxysilane (APTS) is shown in Fig. 8. The successful grafting of APTS onto the nanoparticle surface is evidenced by several characteristic absorption bands. The broad band observed at 1631 cm^{-1} is attributed to the bending vibration of the N–H bond of the free $–NH_2$ groups introduced by APTS. In addition, the absorption bands at 2879 and 2933 cm^{-1} correspond to the symmetric and asymmetric stretching vibrations of the C–H bonds of the propyl chain in the APTS structure, while their bending vibrations are observed around 1465 cm^{-1}.

The stretching vibrations of the C–N bond, typically appearing in the range of 1020–1220 cm^{-1}, are not distinctly resolved in the spectrum due to overlap with the strong and broad absorption band associated with the asymmetric stretching vibration of the Si–O–Si network. The prominent band centered at 1059 cm^{-1} is therefore assigned to Si–O–Si stretching vibrations, confirming the presence of a silica framework on the nanoparticle surface. Characteristic Fe–O vibrations of the magnetite core are also observed at approximately 460 and 585 cm^{-1}, indicating that the crystalline structure of Fe_3O_4 remains intact after surface modification. Furthermore, the band around 3790 cm^{-1} is attributed to the stretching vibration of free hydroxyl (–OH) groups of adsorbed water molecules, while the broad absorption in the 3300–3400 cm^{-1} region is associated with hydrogen-bonded –OH groups.

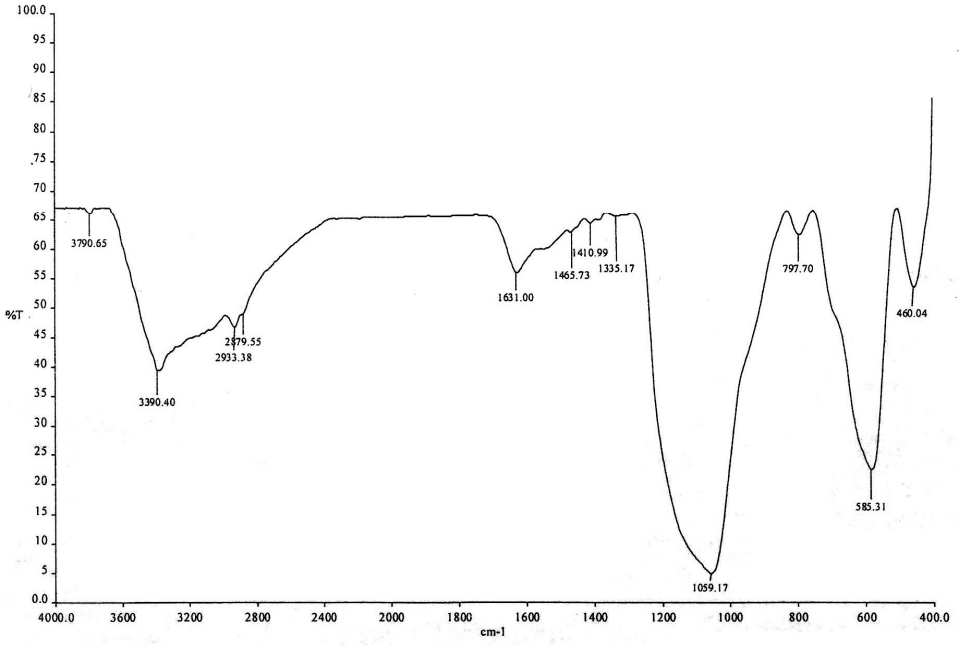

Figure 8: APTS-modified magnetite magnetic nanoparticles' FT-IR spectrum

3.7. FT-IR Spectrum of Bis(acetylacetonato)dioxomolybdenum(VI), $MoO_2(acac)_2$

The FT-IR spectrum of the bis(acetylacetonato)dioxomolybdenum(VI) complex, presented in Fig. 9, exhibits characteristic absorption bands corresponding to the cis-dioxomolybdenum(VI) moiety. The strong bands observed at 960 and 935 cm^{-1} are attributed to the symmetric and asymmetric stretching vibrations of the Mo═O bonds, confirming the presence of the cis-MoO_2 unit. Additionally, the acetylacetonate (acac) ligands give rise to prominent absorption bands at 1585 cm^{-1} and 1506 cm^{-1}, which are assigned to the stretching vibrations of the carbonyl (C═O) group and the conjugated C═C bond, respectively. These features are consistent with the coordination of the acetylacetonate ligands to the molybdenum center.

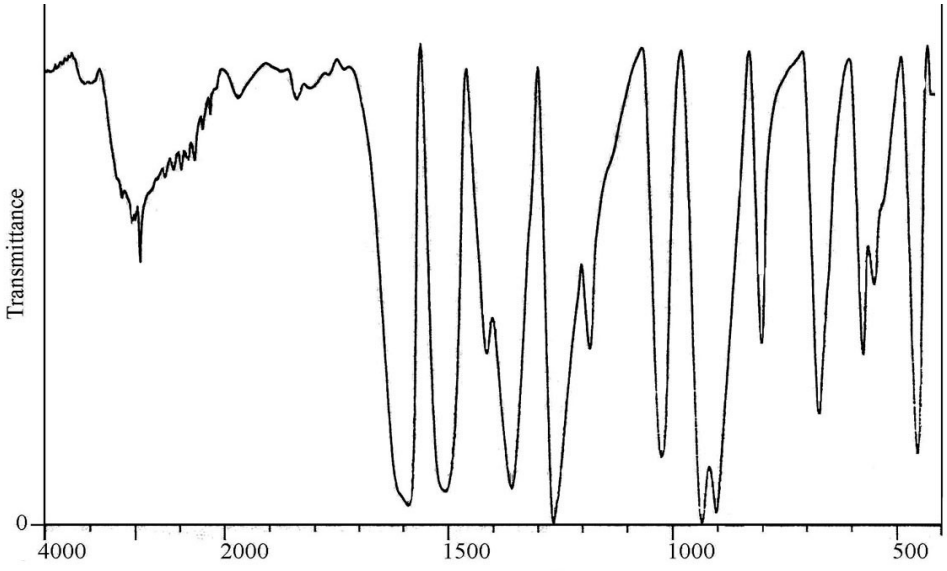

Figure 9: FT-IR spectrum of the complex $MoO_2(acac)_2$

3.8. FT-IR Spectrum of $MoO_2(acac)_2$ Immobilized on Silica-Coated Magnetite Nanoparticles via Aminopropylsilane Groups

Figure 10 displays the FT-IR spectrum of the $MoO_2(acac)_2$ complex immobilized on the surface of magnetite nanoparticles coated with silica. The presence of the silica shell on the iron oxide surface is confirmed by the broad absorption band centered at 1093 cm^{-1}, which is ascribed to the asymmetric stretching vibrations of the Si–O–Si framework. The characteristic bands observed in the 590–460 cm^{-1} region correspond to the stretching vibrations of Fe–O bonds of the magnetite core. Furthermore, the appearance of two adjacent absorption bands in the 960–900 cm^{-1} region is indicative of the cis-dioxomolybdenum (cis-MoO_2) moiety. The presence of these characteristic Mo═O stretching vibrations provides clear evidence for the successful immobilization of the molybdenum complex on the nanoparticle surface.

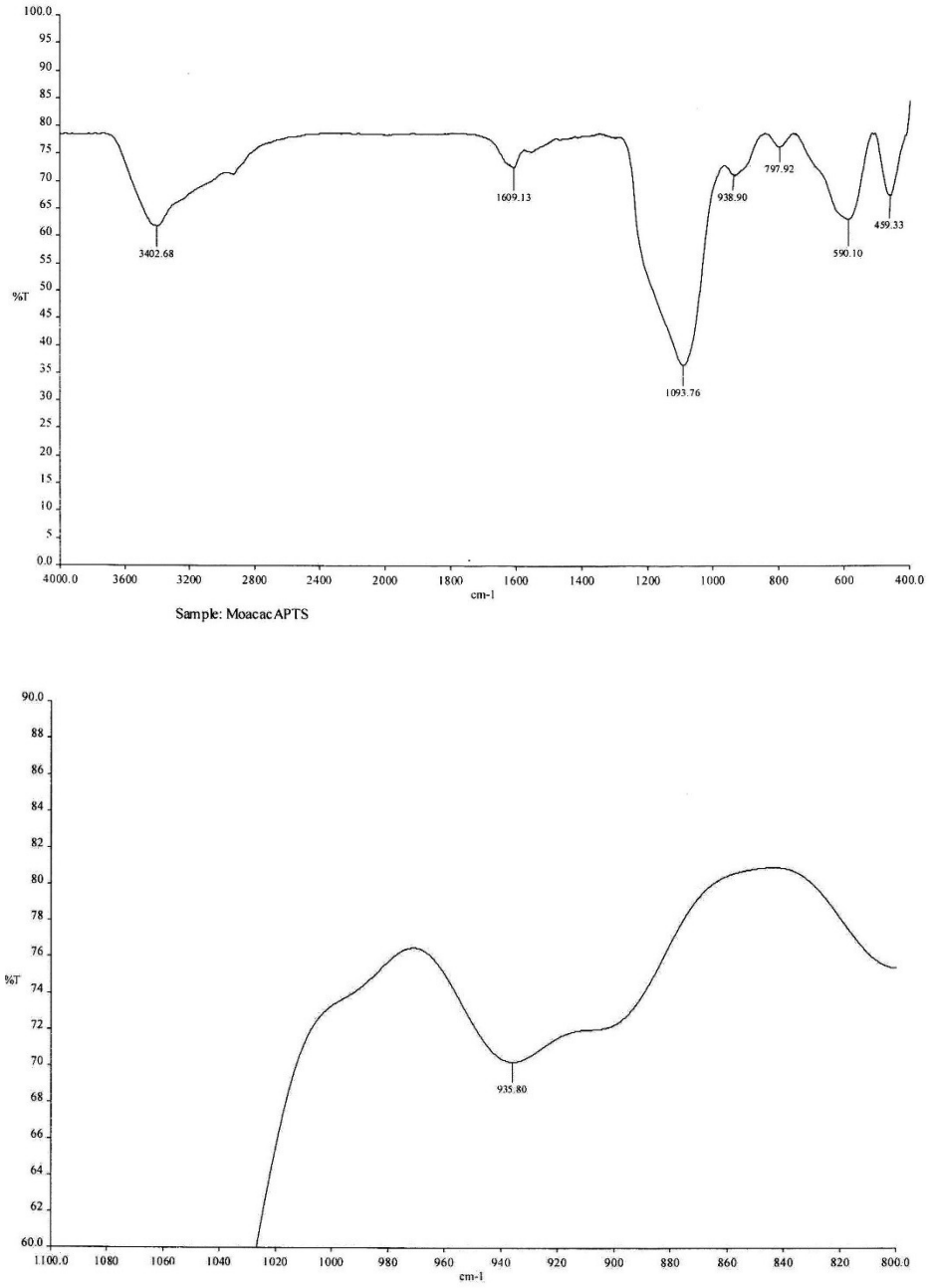

Figure 10: Investigation of FT-IR spectra of $MoO_2(acac)_2$ immobilized on silica-coated magnetite nanoparticles by aminopropylsilane groups

3.9. XRD pattern of molybdenum complex immobilized on nanomagnetite surface

The XRD pattern of the prepared nanoparticles, which is shown in Fig. 11, showed that the synthesized nanoparticles have an inverted spinel crystal structure. In this structure, oxygen anions are distributed in a cubic packed arrangement in the crystal lattice. Additionally, the XRD pattern shows characteristic diffraction peaks at 2θ = 30.1°, 35.5°, 43.1°, 53.4°, 57.0°, and 62.6°, corresponding to the (220), (311), (400), (422), (511), and (440) crystal

planes of magnetite (Fe_3O_4), respectively, which are in good agreement with the standard JCPDS card No. 19-0629.

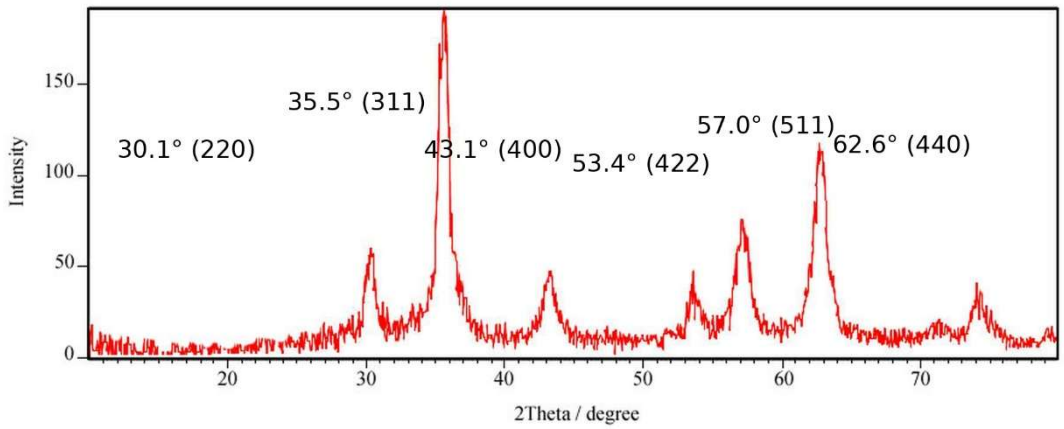

Figure 11: XRD pattern of the bis(acetylacetonato)dioxomolybdenum complex immobilized on the nanomagnetite surface

3.10. VSM Analysis of Bis(acetylacetonato)dioxomolybdenum Immobilized on Magnetite Nanoparticles

Vibrating sample magnetometry (VSM) was used to assess the magnetic characteristics of the bis(acetylacetonato)dioxomolybdenum complex immobilized on the surface of magnetite nanoparticles. Fig. 12 shows the magnetization curve as a function of the applied magnetic field. The magnetization curve's lack of hysteresis suggests single-domain behavior, which validates the nanocomposite's superparamagnetic properties. The saturation magnetization was determined to be approximately 40 $emu \cdot g^{-1}$, which is consistent with reported values for functionalized nanomagnetite systems and indicates that the magnetic responsiveness of the core is preserved after surface modification and complex immobilization.

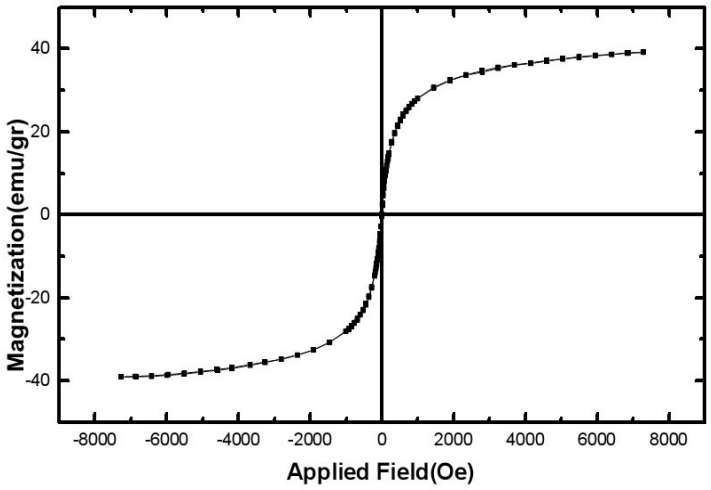

Figure 12: VSM analysis of the bis(acetylacetonato)dioxomolybdenum complex immobilized on the surface of magnetite nanoparticles

3.11. TEM result

By examining the TEM image of the prepared nanoparticles shown in Fig. 13, it was found that the prepared nanomagnetite particles have a spherical shape and the size of these particles is in the range of 10-15 nanometers.

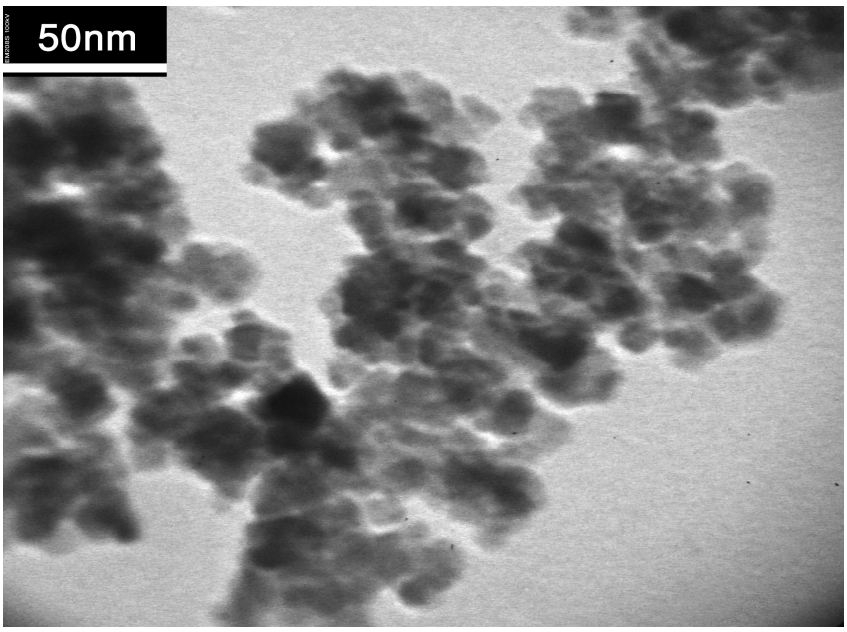

Figure 13: TEM image of the bis(acetylacetonato)dioxomolybdenum complex immobilized on the nanomagnetite surface

3.12. SEM result

As observed in the SEM image shown in Fig. 14, the synthesized magnetite nanoparticles tend to form agglomerates composed of nearly spherical particles that are closely attached to one another. Based on a comparison with the corresponding TEM images, the average particle size of the individual nanoparticles is estimated to be in the range of 10–15 nm.

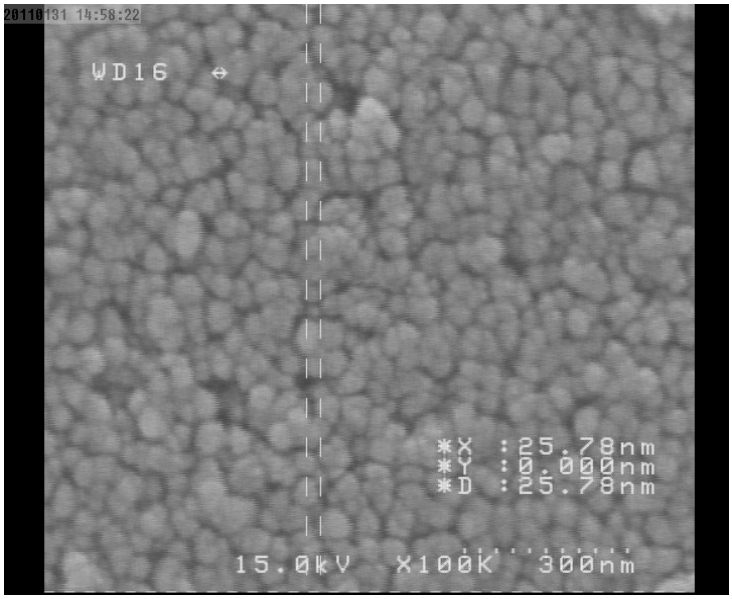

Figure 14: SEM image of the bis(acetylacetonato)dioxomolybdenum complex immobilized on the nanomagnetite surface

3.13. Stabilization of bis(acetylacetonato)dioxomolybdenum complex acac(2MoO_2) on the surface of magnetite nanoparticles

Figure 15 illustrates the general immobilization pathway of the bis(acetylacetonato)dioxomolybdenum(VI) complex on the surface of magnetite nanoparticles. Initially, Fe_3O_4 nanoparticles are coated with a silica shell through the hydrolysis and condensation of tetraethyl orthosilicate (TEOS), generating a hydroxyl-rich SiO_2 surface. These surface silanol groups subsequently react with aminopropyltrimethoxysilane (APTS), resulting in the formation of covalently bonded aminopropyl-functionalized silica-coated magnetite nanoparticles. In the final immobilization step, the $MoO_2(acac)_2$ complex is anchored onto the nanoparticle surface through coordination interactions between the molybdenum center and the surface-exposed amine ($–NH_2$) groups. This interaction leads to the formation of a stable nanocomposite in which the molybdenum complex is firmly immobilized while the magnetic core retains its superparamagnetic behavior. The schematic representation highlights the role of the

silica layer as a spacer and anchoring platform, ensuring effective dispersion of active sites and preventing leaching of the molybdenum complex during subsequent applications.

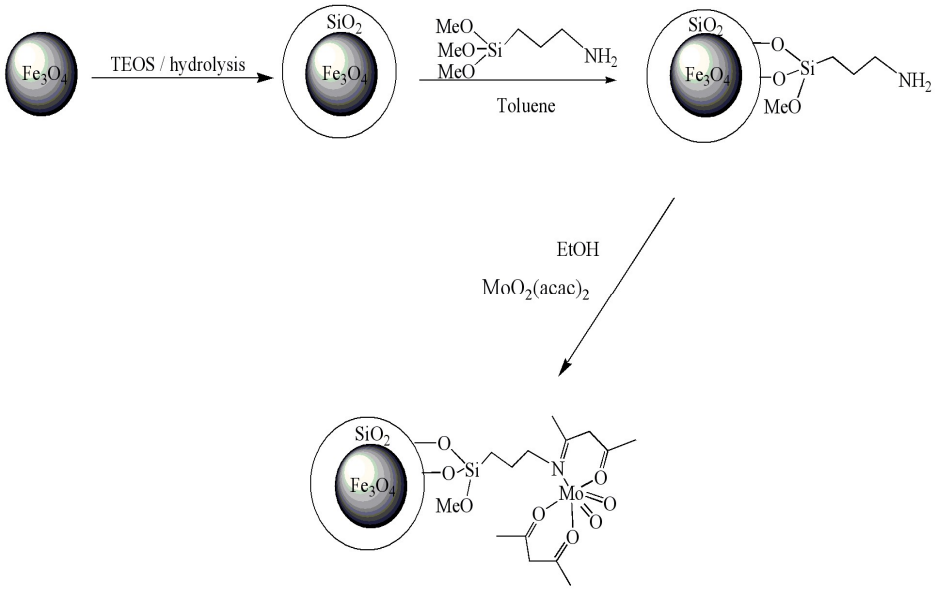

Figure 15: General scheme for immobilization of bis(acetylacetonato)dioxomolybdenum complex on the surface of magnetite nanoparticles

The immobilization of the $MoO_2(acac)_2$ complex onto silica-coated magnetite nanoparticles via aminopropylsilane linkers represents an effective strategy for constructing magnetically recoverable hybrid materials. The successful stepwise surface modification was confirmed by FT-IR spectroscopy through the appearance of characteristic Si–O–Si, N–H, and Mo═O vibrational bands, indicating the formation of a stable coordination environment for the molybdenum complex. The preservation of the inverse spinel structure of Fe_3O_4 and the retention of superparamagnetic behavior, as evidenced by XRD and VSM analyses, demonstrate that the immobilization process does not adversely affect the intrinsic magnetic properties of the magnetite core. Similar approaches have been reported in the literature for the immobilization of molybdenum and other transition-metal complexes on magnetic supports. For instance, Safari et al. immobilized Mo(VI) complexes on silica-coated Fe_3O_4 nanoparticles and reported saturation magnetization values in the range of 35–45 emu·g^{-1} after functionalization, which is in good agreement with the value of approximately 40 emu·g^{-1} observed in the present study [25]. Likewise, Kiasat and coworkers demonstrated that surface functionalization with organosilane linkers significantly enhances the stability of metal complexes on magnetic supports while maintaining sufficient magnetic responsiveness for facile separation [26].

In comparison with studies reporting direct immobilization of molybdenum complexes on bare magnetite surfaces, the use of a silica interlayer in the present work offers distinct

advantages. Bare magnetite-supported systems often suffer from metal leaching and reduced structural stability due to weak surface interactions [27]. The silica shell employed here provides a chemically inert spacer enriched with hydroxyl groups, enabling robust covalent bonding with aminopropylsilane and subsequent coordination of the $MoO_2(acac)_2$ complex. Furthermore, the nanoscale particle size (10–15 nm) observed by TEM is comparable to or smaller than those reported in related studies, which is beneficial for achieving a high surface-to-volume ratio and uniform distribution of active sites [28-30]. Overall, when compared with previously reported molybdenum-based magnetic nanocomposites, the present system combines structural stability, preserved superparamagnetic behavior, and effective immobilization of the Mo(VI) complex. These features highlight its potential applicability in heterogeneous catalysis, biomimetic oxidation systems, and other fields requiring recyclable and magnetically separable functional materials.

4. Conclusions

In this study, a well-defined strategy was successfully developed for the synthesis, surface functionalization, and immobilization of the bis(acetylacetonato)dioxomolybdenum(VI) [$MoO_2(acac)_2$] complex onto magnetite nanoparticles. Magnetite nanoparticles with superparamagnetic behavior were first synthesized via a co-precipitation method and subsequently coated with a silica shell to provide a chemically stable and hydroxyl-rich surface. The introduction of aminopropyl groups enabled efficient coordination-based anchoring of the molybdenum complex onto the nanoparticle surface. Comprehensive characterization using FT-IR, XRD, TEM, SEM, and VSM techniques clearly confirmed the successful surface modification, preservation of the inverse spinel structure of Fe_3O_4, and effective immobilization of the $MoO_2(acac)_2$ complex without significant loss of magnetic properties. The resulting nanocomposite exhibited uniform particle morphology with nanoscale dimensions and retained superparamagnetic behavior, facilitating easy magnetic separation. Overall, this work demonstrates a robust and versatile platform for the stabilization of molybdenum complexes on magnetic supports, offering significant potential for future applications in heterogeneous catalysis, biomimetic systems, and magnetically recoverable functional materials.

References

[1] Wu, W., Wu, Z., Yu, T., Jiang, C., Kim, W.S., *Recent progress on magnetic iron oxide nanoparticles: Synthesis, surface functional strategies and biomedical applications*, Science and Technology of Advanced Materials, 16, 023501, 2015.

[2] Zhao, Y., Zhou, L., & Ren, J. *Application and advances of multifunctional magnetic nanoparticles in cross-disciplinary research: From design to detection, imaging, and therapy*. Coordination Chemistry Reviews, 534, 216590, 2025.

[3] Cornell, R.M., Schwertmann, U., *Iron oxides: Structure, properties, reactions, occurrences and uses*, 3rd ed., Wiley-VCH, 2018.

[4] Al-Rashdi, K. S., Widatallah, H. M., Elzain, M. E., Al-Rawas, A. D., Gismelseed, A. M., Al Ma'Mari, F., & Cespedes, O. *Structural and Mössbauer studies of nanocrystalline Mn2+/Zn2+ codoped Fe3O4 particles*. Interactions, 247(1), 29, 2026.

[5] Valenzuela, R., Magnetic ceramics, Cambridge University Press, 2016.

[6] Roca, A.G., Gutiérrez, L., Gavilán, H., Fortes Brollo, M.E., Veintemillas-Verdaguer, S., Morales, M.P., *Design strategies for shape-controlled magnetic iron oxide nanoparticles*, Advanced Drug Delivery Reviews, 138, 68–104, 2018.

[7] Kettle, S.F.A., *Physical inorganic chemistry: A coordination chemistry approach*, 2nd ed., Oxford University Press, 2017.

[8] Jin, K., Xu, C., Zhao, Y., & Fu, S. *Determination of Fe (II) and Fe (III) in Paramagnetic Matrices Using NMR Relaxometry*. Analytical Chemistry, 97(43), 23802-23810, 2025.

[9] Hille, R., Nishino, T., Bittner, F., *Molybdenum enzymes in higher organisms*, Coordination Chemistry Reviews, 347, 363–394, 2017.

[10] Xiang, L., Wang, Q. W., Wu, W. J., Zheng, N. J., Liu, B. L., Li, Y. W., ... & Li, Q. X. *Overlooked synergisms of flotation organic reagents and toxic metals in water: Formation of tridentate cadmium-xanthate complexes*. Water Research, 124299, 2025.

[11] Schwarz, G., Mendel, R.R., Ribbe, M.W., *Molybdenum cofactors, enzymes and pathways*, Nature, 460, 839–847, 2009.

[12] Seefeldt, L.C., Hoffman, B.M., Dean, D.R., *Mechanism of Mo-dependent nitrogenase*, Annual Review of Biochemistry, 87, 1–30, 2018.

[13] Spatzal, T., Aksoyoglu, M., Zhang, L., Andrade, S.L.A., Schleicher, E., Weber, S., Rees, D.C., Einsle, O., *Evidence for interstitial carbon in nitrogenase FeMo cofactor*, Science, 334, 940–940, 2011.

[14] Qaim, S.M., *The present status of medical radionuclide production*, Radiochimica Acta, 105, 737–750, 2017.

[15] Zhao, H., Shu, J., Lin, F., Wang, J., Luo, J., Yang, Y., & Chen, M. *A novel method for desulfurization of electrolytic manganese residue using $KHCO_3$: Mechanisms of sulfate transformation and heavy metal mineralization*. Process Safety and Environmental Protection, 107958, 2025.

[16] Haynes, W.M., CRC handbook of chemistry and physics, 97th ed., CRC Press, 2016.

[17] Thamer, B. M., Al-aizari, F. A., Abdo, H. S., & Altaleb, H. A. *Single-step preparation of copper nanoparticle-enhanced activated carbon for anionic dye adsorption*. Colloids and Surfaces A: Physicochemical and Engineering Aspects, 711, 136359, 2025.

[18] Wu, W., Wu, Z., Yu, T., Jiang, C., Kim, W.S., *Recent progress on magnetic iron oxide nanoparticles: Synthesis, surface functional strategies and biomedical applications*, Science and Technology of Advanced Materials, 16, 023501, 2016.

[19] Pasieczna-Patkowska, S., Cichy, M., & Flieger, J. *Application of Fourier transform infrared (FTIR) spectroscopy in characterization of green synthesized nanoparticles*. Molecules, 30(3), 684, 2025.

[20] Lu, A.-H., Salabas, E.L., Schüth, F., *Magnetic nanoparticles: Synthesis, protection, functionalization, and application*, Angewandte Chemie International Edition, 46, 1222–1244, 2007.

[21] Assi, G. A., Ali, R., Kazemi, M., M, R. M., Al-Hasnaawei, S., Ray, S., ... & Javahershenas, R. *Heterocyclic Synthesis Using Magnetic Bromine and Iodine Nanoparticles*. Chemistry–An Asian Journal, 20(23), e70409, 2025.

[22] Kiasat, A.R., Davarpanah, J., *Surface functionalization of silica-coated magnetic nanoparticles with organosilanes and their applications*, Applied Surface Science, 387, 719–725, 2016.

[23] Safari, J., Gandomi-Ravandi, S., *Immobilization of molybdenum(VI) complexes on functionalized magnetic nanoparticles: Synthesis and characterization*, Journal of Molecular Catalysis A: Chemical, 426, 1–9, 2017.

[24] Florio, F., Ferlazzo, A., Bonforte, S., Nicotra, G., Neri, G., Pinkas, I., ... & Gulino, A. *Unveiling the sensing ability of new MoS 2 nanoparticles: from fundamental insights into practical applications for nitrites*. Journal of Materials Chemistry C, 13(22), 11214-11222, 2025.

[25] Safari, J., Gandomi-Ravandi, S., *Immobilization of molybdenum(VI) complexes on silica-coated magnetic nanoparticles: Synthesis and characterization*, Journal of Molecular Catalysis A: Chemical, 393, 268–275, 2014.

[26] Kiasat, A.R., Davarpanah, J., *Magnetic nanoparticle-supported metal complexes: Preparation, characterization and catalytic applications*, Applied Organometallic Chemistry, 27, 283–290, 2013.

[27] Polshettiwar, V., Varma, R.S., *Green chemistry by nano-catalysis*, Green Chemistry, 12, 743–754, 2010.

[28] Laurent, S., Forge, D., Port, M., Roch, A., Robic, C., Vander Elst, L., Muller, R.N., *Magnetic iron oxide nanoparticles: Synthesis, stabilization, vectorization, physicochemical characterizations, and biological applications*, Chemical Reviews, 108, 2064–2110, 2008.

[29] Zhang, J., Lei, N., Jia, Y., Guo, S., Ouyang, L., & Xiao, X. *π–π electron conjugation-assisted synthesis of a robust heterostructured CoO–MoO 2 catalyst: accelerated ammonia borane hydrolysis for hydrogen evolution*. Nanoscale, 17(45), 26238-26247, 2025.

[30] Liu, J., Liu, C., Qiu, X., Zhang, T., Gao, S., Song, X., & Chen, F. *CeF3-Accelerated surface reconstruction of MoO_2 nanosheets into coral-like CeF_3/MoO_2 composites enhances the oxygen evolution reaction for efficient water splitting*. Journal of Colloid and Interface Science, 683, 1057-1066, 2025.